JOURNAL OF SOLID STATE CHEMISTRY 108, 291–298 (1994)

The Monophosphate $Pb_2V_2VO(PO_4)_4$: A Tunnel Structure with the Mixed Valence V(III)–V(IV)

A. Leclaire, J. Chardon, A. Grandin, M. M. Borel, and B. Raveau

Laboratoire CRISMAT, URA 1318 associé au CNRS-ISMRA, Université de Caen, Boulevard du Maréchal Juin, 14050 Caen Cedex, France

Received December 7, 1992; in revised form June 2, 1993; accepted June 4, 1993

A new vanadium monophosphate, $Pb_2V_2VO(PO_4)_4$, characterized by the mixed valence V(III)–V(IV), has been synthesized. It crystallizes in the space group $C2/c$ with a = 17.747(2) Å, b = 18.051(2) Å, c = 9.344(1) Å, and β = 117.03(1)°. This structure can be described from the $[V_2P_4O_{16}]_\infty$ framework built up from corner-sharing PO_4 tetrahedra and VO_6 octahedra. This host lattice consists of cross-linked $[VPO_8]_\infty$ chains forming $[VP_2O_{10}]_\infty$ layers parallel to (001); the whole $[V_2P_4O_{16}]_\infty$ framework results from the stacking along [104] of identical $[VP_2O_{10}]_\infty$ layers. This three-dimensional framework delimits tunnels running along the [001] and [102] where Pb^{2+} ions are located; it forms also large tunnels running along [110] and [1$\bar{1}$0] which are obstructed by vanadyl ions. The latter form VO_5 pyramids with the surrounding oxygens; each VO_5 pyramid shares one edge with one PO_4 tetrahedron, forming VPO_7 units. Bond valence calculations show that V(IV) and V(III) species are distributed in an ordered way, in VO_5 pyramids and VO_6 octahedra, respectively, whereas lead is in the divalent state. The Pb(II) cations, which exhibit two kinds of coordination, 7 and 8, show a stereoactivity of their $6s^2$ lone pair.

INTRODUCTION

The great ability of vanadium to form VO_n polyhedra with various configurations—tetrahedral, pyramidal, and octahedral—and large distortions has allowed a rich family of vanadium phosphates to be developed. Besides the phosphates characterized by a well-defined oxidation state of vanadium, i.e., V(V) (1–4), V(IV) (5–19), and V(III) (20–24), mixed-valent vanadium phosphates are of interest for their possibility of electron transfer that can induce particular physical properties. Several phosphates characterized by the mixed valence V(V)–V(IV) were recently isolated in the form either of hydrated phases $Na_x VOPO_4 \cdot nH_2O$ (25–26) or of anhydra phosphates such as $RbV_3P_4O_{17+x}$ (27), $KV_3P_4O_{17}$ (28), and $Rb_6V_6P_6O_{31}$ (29). The recent exploration of phosphates involving the mixed valence V(IV)–V(III) has allowed three new phosphates—$KV_3P_4O_{16}$ (30), $V_3P_4O_{15}$ (31), and $Cd_5V_3P_6O_{25}$ (32)—to be synthesized. The study of such systems characterized by the mixed valence V(IV)–V(III) appears to be very promising, since very few systems have been investigated until now. We report here on a new monophosphate, $Pb_2V_2VO(PO_4)_4$, with a tunnel structure built up from V(III) octahedra and V(IV) tetragonal pyramids.

SYNTHESIS

Single crystals of vanadium phosphate were grown from a mixture of nominal composition $PbV_2P_2O_{10}$. First, $H(NH_4)_2PO_4$, $Pb(CH_3COO)_2 \cdot 3H_2O$, and V_2O_5 were mixed in an agate mortar in adequate ratio to the composition $PbV_{0.8}P_2O_{10}$, and heated at 650 K in a platinum crucible to decompose the ammonium phosphate and the lead acetate. In a second step, the resulting mixture was then added to the required amount of vanadium (0.2 mol), placed in an alumina tube, and sealed in an evacuated silica ampoule, then heated for 1 day at 1225 K and cooled at 1 K per hr to 1075 K. The sample was finally quenched to room temperature. When the ampoule was opened, we obtained a mixture in which some green crystals were isolated. The composition deduced from the structural determination $Pb_2V_3P_4O_{17}$ was confirmed by microprobe analysis. Subsequently, a reaction to prepare $Pb_2V_3P_4O_{17}$ was performed. The powder X-ray diffraction pattern of the phase was indexed in a monoclinic cell (Table 1), in agreement with the parameters obtained from the single crystal study.

STRUCTURE DETERMINATION

A green crystal with dimensions 0.077 × 0.077 × 0.039 mm was selected for the structure determination. The cell parameters reported in Table 2 were determined and refined by diffractometric techniques at 293 K with a least-squares refinement based upon 25 reflections with $18° < \theta < 22°$. The systematic absences $h + k = 2n + 1$ for all the hkl, $l = 2n + 1$ for $h0l$, and $k = 2n + 1$ for $0k0$ are consistent with the space groups Cc and $C2/c$. The Patterson function shows $u0w$ and $u1/2w$ peaks which

0022-4596/94 $6.00

TABLE 1
Interrecticular Distances

h	k	l	d_{calc} Å	d_{obs} Å	I
1	1	0	11.893	11.910	19
0	2	0	9.025	9.036	16
2	0	0	7.904	7.918	13
2	2	0	5.946	5.940	50
1	3	0	5.623	5.631	8
3	1	−1	5.522	5.532	11
1	1	−2	4.428	4.434	34
3	3	−1	4.176	4.182	11
0	0	2	4.162	4.167	61
2	2	−2	4.138	4.144	71
1	3	−2	3.638	3.643	14
4	2	0	3.620	3.626	14
1	1	2	3.566	3.569	15
3	3	−2	3.537	3.542	11
1	5	0	3.519	3.524	11
1	5	−1	3.366	3.370	12
5	1	−2	3.301	3.307	10
2	4	−2	3.241	3.245	7
3	3	1	3.182	3.186	45
4	4	−1	3.162	3.168	95
1	5	1	3.130	3.134	27
5	1	0	3.114	3.118	36
1	3	2	3.113		
3	5	−1	3.065	3.063	17
3	1	−3	3.060		
0	4	2	3.059		
4	4	0	2.973	2.970	100
2	2	2	2.966		
4	4	−2	2.941	2.946	36
5	3	−2	2.932	2.931	26
2	2	−3	2.927		
2	6	0	2.812	2.815	35
2	6	−1	2.805	2.808	41
5	3	0	2.799		
3	5	−2	2.784	2.786	16
6	2	−2	2.761	2.764	32
3	3	−3	2.759		
0	2	3	2.652	2.655	23
5	1	1	2.564	2.568	18
1	5	2	2.563		11
4	4	1	2.538	2.531	11
6	2	0	2.529		
2	6	−2	2.527		
3	3	2	2.478	2.482	15
1	7	1	2.385	2.388	11

are only compatible with the $C2/c$ space group. The data were collected on a CAD-4 Enraf–Nonius diffractometer with the data collection parameters reported in Table 2. The reflections were corrected for Lorentz and polarization effects. Gaussian absorption correction was performed.

The structure was solved by the heavy atom method. The refinement of the coordinates and the anisotropic thermal factors of the heavy atoms and the isotropic thermal factors of the oxygen atoms led to $R = 0.041$, $R_W = 0.046$, and to the atomic parameters of Table 3.

DESCRIPTION OF THE STRUCTURE AND DISCUSSION

The structure of the phosphate $Pb_2V_3P_4O_{17}$ is built up from single PO_4 tetrahedra sharing their corners with single VO_6 octahedra, and one edge with VO_5 pyramids. Thus, this monophosphate can be formulated $Pb_2V_2(VO)(PO_4)_4$, where VO represents the vanadyl ion. The view of the structure along [001] (Fig. 1) and along [102] (Fig. 2) shows that these polyhedra delimit tunnels running along these directions, where the Pb(2) and Pb(1) cations are located, respectively. These two projections of the structure, although they show the existence of tunnels, do not allow a clear and simple description to be given. A better understanding of this framework can be obtained by considering a one-unit-cell-thick layer parallel to the (001) plane (Fig. 3). From this projection, one observes clearly $[VPO_8]_\infty$ chains running along [110] and [1$\bar{1}$0] in which one VO_6 octahedron alternates with one PO_4 tetrahedron, as observed in many phosphates of transition elements (33).

In fact, a rather simple description of this structure can be proposed by considering only the $[V_2P_4O_{16}]_\infty$ host lattice built up from corner-sharing PO_4 tetrahedra and VO_6 octahedra. The arrangement of the polyhedra shown in Fig. 3 allows the $[V_2P_4O_{16}]_\infty$ framework to be described from the connection of $[VPO_8]_\infty$ chains only. Indeed, one

TABLE 2
Summary of Crystal Data, Intensity Measurements, and Structure Refinement Parameters for $Pb_2V_3P_4O_{17}$

1. Crystal data	
Space group	$C\,2/c$
Cell dimensions	a = 17.747(2) Å
	b = 18.051(2) Å, β = 117.03(1)
	c = 9.344(1) Å
Volume	2666(9) Å^3
Z	8
d_{calc}	4.80
2. Intensity measurements	
λ (MoK$\bar{\alpha}$)	0.71073 Å
Scan mode	$\omega - 4/3\,\theta$
Scan width (°)	1.00 + 0.35 tan θ
Slit aperture (mm)	1.18 + tan θ
Max θ (°)	42
Standard reflections	3 every 3000 sec
Measured reflections	9886
Reflections with $I > 3\sigma$	2613
μ (mm^{-1})	27.9
Range h	−33 + 33
k	0 + 34
l	0 + 17
3. Structure solution and refinement	
Parameters refined	151
Agreement factors	R = 0.041, R_w = 0.046
Δ/σ max	<0.004

TABLE 3
Positional Parameters and Their Estimated Standard Deviations

Atom	x	y	z	B(Å^2)
Pb(1)	0.11296(3)	0.12510(3)	0.01898(6)	0.920(7)
Pb(2)	0.22976(3)	0.47431(3)	0.46871(6)	0.991(7)
V(1)	0.4472(1)	0.2102(1)	0.4457(2)	0.48(3)
V(2)	0.2469(1)	0.3097(1)	0.2474(2)	0.35(3)
V(3)	0.	0.0612(2)	0.25	0.37(4)
V(4)	0.5	0.0559(2)	0.25	0.42(4)
P(1)	0.1385(2)	0.1989(2)	0.3627(3)	0.43(5)
P(2)	0.3879(2)	0.4437(2)	0.3419(3)	0.35(5)
P(3)	0.3324(2)	0.1657(2)	0.1492(4)	0.50(5)
P(4)	0.0830(2)	0.4212(2)	0.1295(3)	0.41(5)
O(1)	0.5041(7)	0.2729(6)	0.422(1)	1.4(2)[a]
O(2)	0.3285(5)	0.2246(6)	0.270(1)	0.7(1)[a]
O(3)	0.4131(6)	0.2441(6)	0.601(1)	1.1(2)[a]
O(4)	0.4256(5)	0.1401(5)	0.261(1)	0.6(1)[a]
O(5)	0.5147(6)	0.1365(6)	0.597(1)	1.2(2)[a]
O(6)	0.1738(5)	0.3924(5)	0.240(1)	0.7(1)[a]
O(7)	0.2899(6)	0.3316(6)	0.482(1)	1.0(1)[a]
O(8)	0.1727(5)	0.2303(6)	0.251(1)	0.7(1)[a]
O(9)	0.1804(6)	0.2975(6)	0.003(1)	1.0(1)[a]
O(10)	0.3384(5)	0.3750(6)	0.251(1)	0.9(1)[a]
O(11)	0.0364(5)	0.0732(5)	0.495(1)	0.5(1)[a]
O(12)	0.0809(5)	−0.0204(5)	0.272(1)	0.6(1)[a]
O(13)	0.0882(6)	0.1325(6)	0.265(1)	0.9(1)[a]
O(14)	0.5776(5)	−0.0138(5)	0.234(1)	0.8(1)[a]
O(15)	0.4185(6)	0.0499(6)	0.023(1)	1.1(1)[a]
O(16)	0.3290(6)	0.4991(6)	0.367(1)	0.9(1)[a]
O(17)	0.2708(6)	0.1026(6)	0.123(1)	0.8(1)[a]

Note. Anisotropically refined atoms are given in the form of the isotropic equivalent displacement parameter defined as $B = 4/3\ [\beta_{11}\ a^2 + \beta_{22}\ b^2 + \beta_{33}\ c^2 + \beta_{12}\ ab \cos \lambda + \beta_{13}\ ac \cos \beta + \beta_{23}\ bc \cos \alpha]$.

[a] Atoms were refined isotropically.

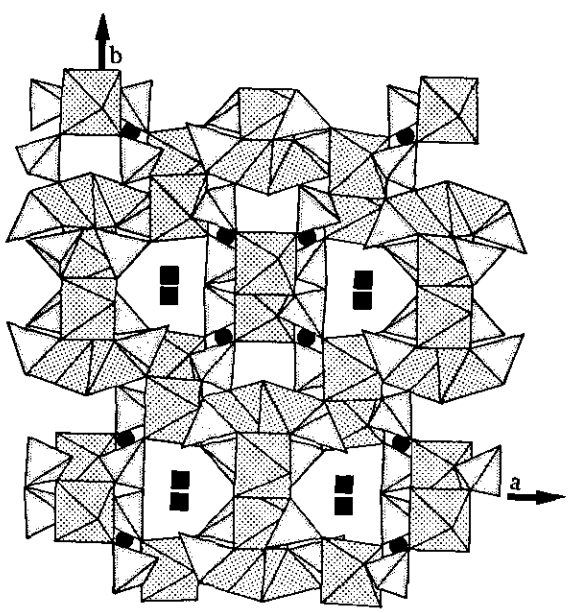

FIG. 1. Projection of the structure of $Pb_2V_3P_4O_{17}$ along $\vec{c}$ showing the tunnels containing Pb(2) (■).

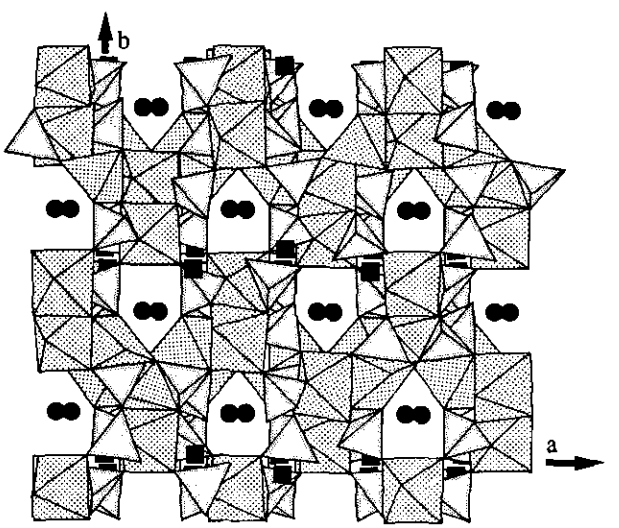

FIG. 2. Projection of $Pb_2V_3P_4O_{17}$ structure along [102] showing the tunnels filled with Pb(1) (●).

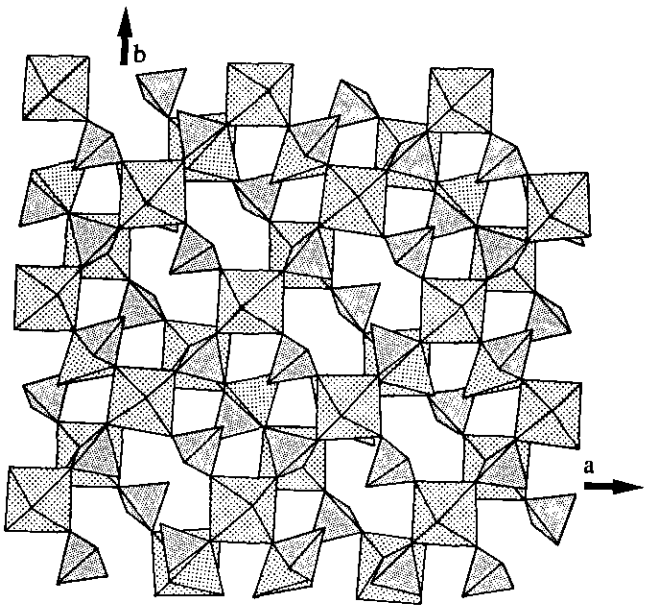

FIG. 3. One unit cell thick layer parallel to the (001) plane.

observes that the whole $[V_2P_4O_{16}]_\infty$ framework consists of identical $[VP_2O_{10}]_\infty$ layers parallel to (001), formed of interpenetrating cross-linked $[VPO_8]_\infty$ chains running along [110] and [1$\bar{1}$0], respectively (Fig. 4). Along the [104] direction, perpendicular to the (001) plane, the stacking of two successive $[VP_2O_{10}]_\infty$ layers leads to $[V_2P_4O_{18}]_\infty$ double layers (Fig. 5). These double layers result from the association of one $[VPO_8]_\infty$ chain of a single $[VP_2O_{10}]_\infty$ layer with another parallel chain of the next single layer, forming double $[V_2P_2O_{14}]_\infty$ chains (Fig. 5); such double $[V_2P_2O_{14}]_\infty$ chains in which one octahedron of one $[VPO_8]_\infty$ chain shares its corner with one PO_4 tetrahedron of the other $[VPO_8]_\infty$ chain have been previously observed in molybdenum and vanadium phosphates such as $NaMo_3P_3O_{16}$ (34) and β-VPO_5 (1). The whole $[V_2P_4O_{16}]_\infty$ framework is then described by the stacking of identical $[V_2P_4O_{18}]_\infty$ double layers along the [104] direction in such a way that one $[VPO_8]_\infty$ chain of one double layer $[V_2P_4O_{18}]_\infty$ running along [110] is connected with a similar chain of the next double layer, but oriented at 90°, i.e., with a $[VPO_8]_\infty$ chain running along [1$\bar{1}$0] (Fig. 5).

The view of the structure along [110] and [1$\bar{1}$0] (Fig. 6) shows that $[V_2P_4O_{16}]_\infty$ framework delimits large six-sided tunnels running along these directions. In fact, these tunnels are obstructed by vanadyl groups, which sit on the border of the $[V_2P_2O_{14}]_\infty$ double chains forming VO_5 pyramids (Fig. 7). The latter share one edge of their basal plane with a PO_4 octahedron of the $[V_2P_2O_{14}]_\infty$ double chains (Fig. 7), forming VPO_7 units; the other two apices of the basal plane of these pyramids are shared with the

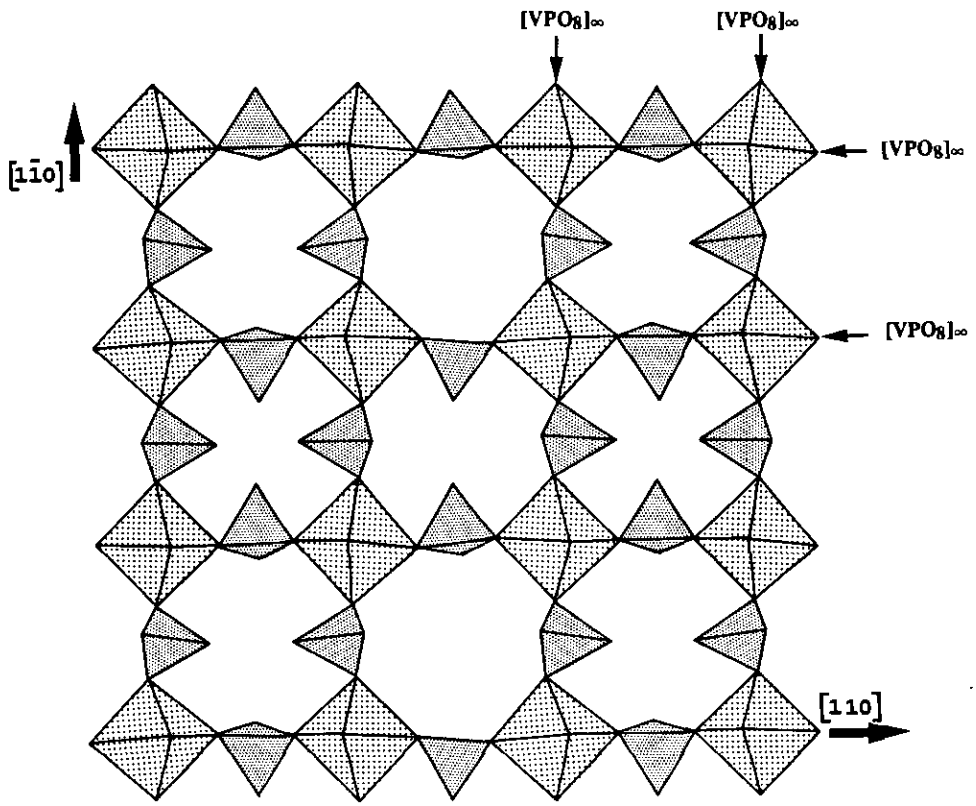

FIG. 4. The $[VP_2O_9]_\infty$ layer formed of interpenetration cross linked $[VPO_8]_\infty$ chains.

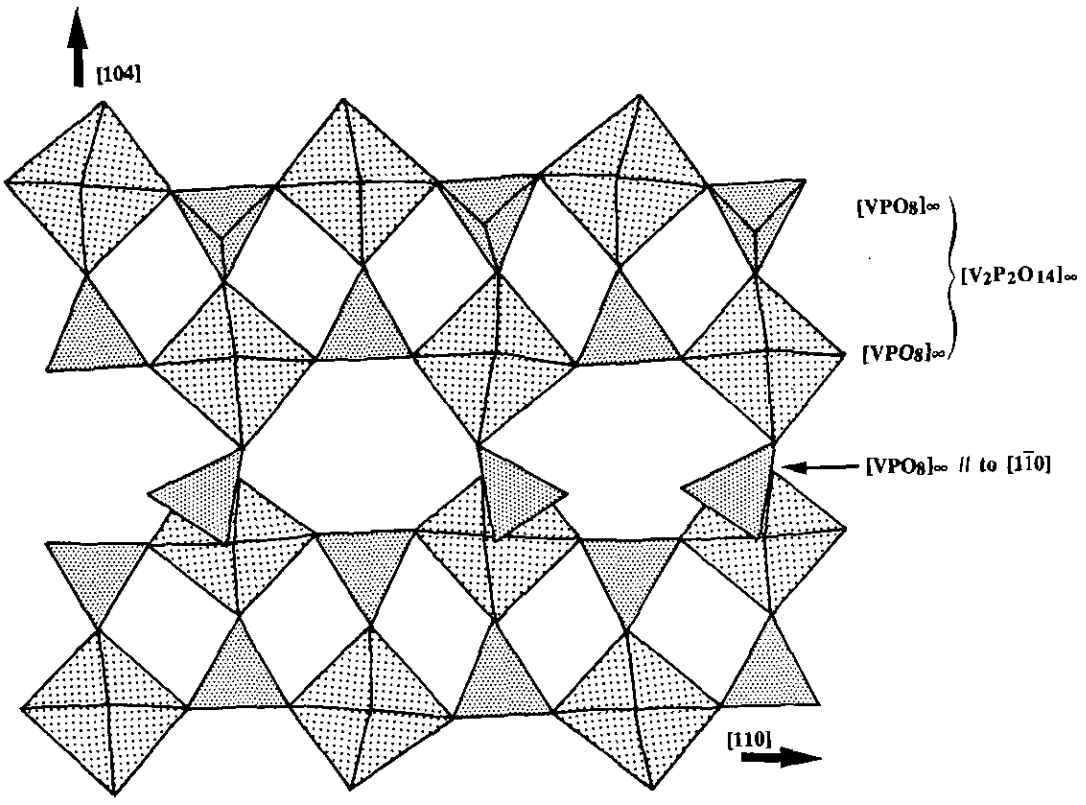

FIG. 5. Stacking of the $[VP_2O_{10}]_\infty$ layer along the [104] direction. The $[VP_2O_{10}]_\infty$ layers perpendicular to the plane of projection are represented by $[VPO_8]_\infty$ chains running along [110] at two different levels. Two successive $[VP_2O_{10}]_\infty$ layers form double $[V_2P_4O_{18}]_\infty$ layers represented by double $[V_2P_4O_{14}]_\infty$ chains. The connection between two double $[V_2P_4O_{18}]_\infty$ layers is ensured by $[VPO_8]_\infty$ chains perpendicular to the projection, i.e., running along [110].

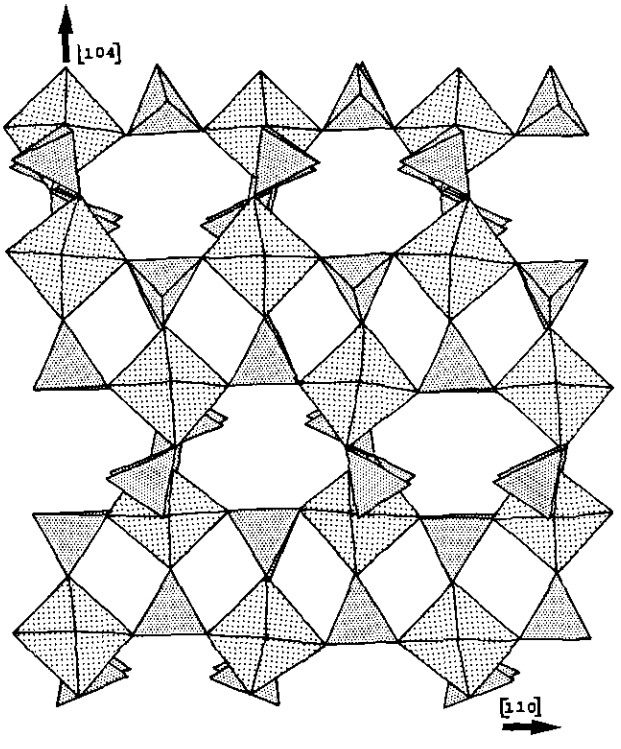

FIG. 6. Projection of the $[V_2P_4O_{16}]_\infty$ framework along [110] or [1$\bar{1}$0].

PO_4 tetrahedra of two $[V_2P_2O_{14}]_\infty$ chains running at 90°, the fifth apical apex being free.

One important characteristic of this phosphate is that the VO_6 octahedra are highly distorted as shown by O–O distances ranging from 2.52 to 3.06 Å and by O–V–O angles from 78.8 to 94.4°. Nevertheless the V–O distances spread over a rather limited range (1.92–2.09 Å) (Table 4).

This comes from the fact that some of the oxygen atoms of the VO_6 octahedra are triply bonded, i.e., are shared between three polyhedra: one VO_6 octahedron, one PO_4 tetrahedron, and one VO_5 pyramid. This is indeed the case of the V(2) and V(4) octahedra (Table 4) which are linked to six PO_4 tetrahedra, but which share, in addition, one and two corners with VO_5 pyramids, respectively. Although they are linked to six PO_4 tetrahedra and do not share corners with VO_5 pyramids, the V(3) octahedra are also strongly distorted.

The distortion of the VO_5 pyramids is spectacular compared to that of other vanadium phosphates, with O–O distances ranging from 2.33 to 2.91 Å (Table 4). Their base has a trapezoidal shape, whose small edge is shared with the PO_4 tetrahedron in the VPO_7 unit; nevertheless its basal V–O distances (1.91–2.03 Å) as well as its short apical V–O bond of 1.60 Å are close to those generally observed in VO_5 pyramids for other phosphates.

TABLE 4
Main Interatomic Distances (Å) Angles (°)

V(1)	O(1)	O(2)	O(3)	O(4)	O(5)
O(1)	1.60(1)	2.91(2)	2.85(2)	2.84(2)	2.91(2)
O(2)	106.8(5)	2.01(1)	2.78(1)	2.33(1)	3.69(2)
O(3)	108.4(6)	90.3(4)	1.91(1)	3.78(2)	2.66(2)
O(4)	102.1(5)	70.3(4)	147.5(5)	2.03(1)	2.80(1)
O(5)	111.8(5)	139.8(5)	88.3(5)	90.3(4)	1.91(1)

V(2)	O(2)	O(6)	O(7)	O(8)	O(9)	O(10)
O(2)	2.06(1)	4.01(2)	3.06(2)	2.69(1)	2.98(1)	2.73(2)
O(6)	176.5(8)	1.96(1)	2.52(1)	2.93(2)	2.84(1)	2.90(1)
O(7)	97.9(4)	78.8(4)	2.01(1)	2.87(2)	4.04(2)	2.78(2)
O(8)	84.2(4)	96.8(4)	92.8(4)	1.96(1)	2.67(2)	3.94(2)
O(9)	93.1(4)	90.4(4)	168.1(4)	83.7(4)	2.05(1)	3.05(1)
O(10)	84.8(4)	94.2(5)	88.0(4)	169.0(4)	97.6(4)	2.00(1)

V(3)	O(11)	O(11^{i})	O(12)	O(12^{i})	O(13)	O(13^{i})
O(11)	2.09(1)	4.16(2)	3.06(2)	2.95(1)	2.91(1)	2.66(1)
O(11^{i})	168.1(5)	2.09(1)	2.95(2)	3.06(2)	2.66(2)	2.91(2)
O(12)	96.6(4)	92.1(4)	2.00(1)	2.71(2)	2.77(2)	3.98(2)
O(12^{i})	92.1(4)	96.6(4)	85.3(6)	2.00(1)	3.98(2)	2.77(2)
O(13)	90.9(4)	81.3(4)	87.9(4)	172.8(4)	1.98(1)	3.02(2)
O(13^{i})	81.3(4)	90.9(4)	172.8(4)	87.9(4)	99.0(6)	1.98(1)

V(4)	O(4)	O(4^{ii})	O(14)	O(14^{ii})	O(15)	O(15^{ii})
O(4)	2.05(1)	2.74(2)	3.96(2)	2.78(1)	2.71(2)	3.05(2)
O(4^{ii})	84.0(5)	2.05(1)	2.78(2)	3.96(2)	3.05(2)	2.71(2)
O(14)	172.8(4)	88.9(4)	1.92(1)	2.91(2)	2.85(2)	2.52(2)
O(14^{ii})	88.9(4)	172.8(4)	98.3(6)	1.92(1)	2.52(2)	2.85(2)
O(15)	85.4(4)	99.4(4)	94.6(4)	81.2(4)	1.95(1)	3.90(2)
O(15^{ii})	99.4(4)	85.4(4)	81.2(4)	94.6(4)	173.7(7)	1.95(1)

P(1)	O(3^{iii})	O(7^{iii})	O(8)	O(13)
O(3^{iii})	1.52(1)	2.51(2)	2.52(2)	2.56(2)
O(7^{iii})	111.0(6)	1.53(1)	2.53(2)	2.46(1)
O(8)	111.7(6)	111.2(6)	1.53(1)	2.36(2)
O(13)	114.8(6)	107.1(6)	100.7(6)	1.53(1)

P(2)	O(10)	O(11^{iii})	O(12^{iv})	O(16)
O(10)	1.54(1)	2.58(1)	2.43(1)	2.53(2)
O(11^{iii})	114.4(6)	1.54(1)	2.52(1)	2.51(1)
O(12^{iv})	104.4(5)	109.8(5)	1.54(1)	2.50(1)
O(16)	110.6(6)	109.2(6)	108.2(6)	1.54(1)

P(3)	O(2)	O(4)	O(9^{v})	O(17)
O(2)	1.57(1)	2.33(1)	2.51(1)	2.55(1)
O(4)	95.7(5)	1.57(1)	2.58(1)	2.54(1)
O(9^{v})	110.2(6)	115.0(6)	1.49(1)	2.51(1)
O(17)	111.1(6)	111.0(6)	113.1(6)	1.52(1)

P(4)	O(5^{vi})	O(6)	O(14^{vii})	O(15^{v})
O(5^{vi})	1.52(1)	2.57(1)	2.55(2)	2.51(2)
O(6)	113.2(6)	1.56(1)	2.39(1)	2.48(2)
O(14^{vii})	111.8(6)	100.2(5)	1.56(1)	2.52(2)
O(15^{v})	112.3(6)	108.3(6)	110.6(6)	1.50(1)

Pb(1)–O(1^{vi})	2.51(1)	Pb(2)–O(6)	2.41(1)
Pb(1)–O(8)	2.71(1)	Pb(2)–O(7)	2.77(1)
Pb(1)–O(10^{v})	3.01(1)	Pb(2)–O(14^{vii})	2.60(1)
Pb(1)–O(11^{i})	2.76(1)	Pb(2)–O(15^{iv})	3.00(1)
Pb(1)–O(12^{viii})	2.84(1)	Pb(2)–O(16)	2.40(1)
Pb(1)–O(13)	2.53(1)	Pb(2)–O(17^{iv})	2.47(1)
Pb(1)–O(16^{ix})	2.53(1)	Pb(2)–O(12^{iii})	3.23(1)
Pb(1)–O(17)	2.55(1)		

i	$-x$	y	$\frac{1}{2} - z$
ii	$1 - x$	y	$\frac{1}{2} - z$
iii	$\frac{1}{2} - x$	$\frac{1}{2} - y$	$1 - z$
iv	$\frac{1}{2} - x$	$\frac{1}{2} + y$	$\frac{1}{2} - z$
v	$\frac{1}{2} - x$	$\frac{1}{2} - y$	$-z$
vi	$-\frac{1}{2} + x$	$\frac{1}{2} - y$	$-\frac{1}{2} + z$
vii	$-\frac{1}{2} + x$	$\frac{1}{2} + y$	z
viii	x	$-y$	$-\frac{1}{2} + z$
ix	$\frac{1}{2} - x$	$-\frac{1}{2} + y$	$\frac{1}{2} - z$

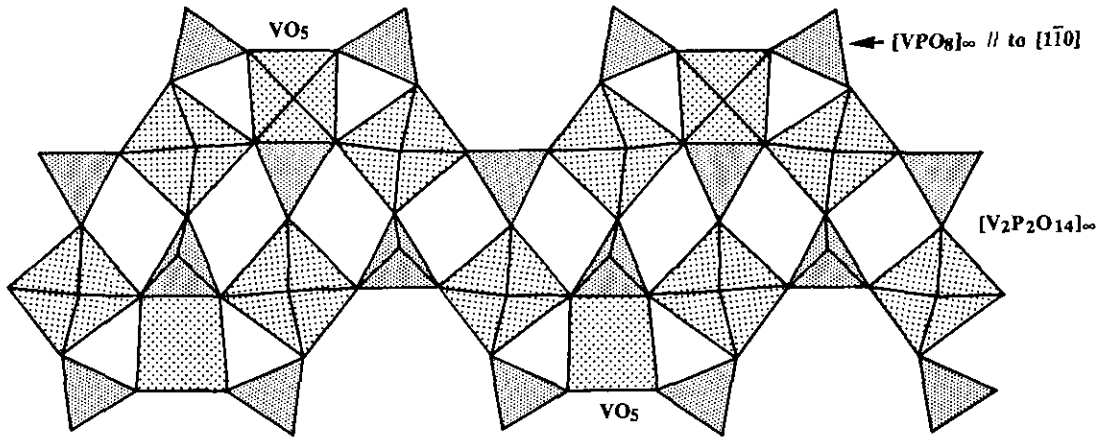

FIG. 7. The VO_5 pyramids located at the border of the $[V_2P_4O_{14}]_\infty$ chains, sharing one edge with a PO_4 tetrahedron and two corners with PO_4 tetrahedra of $[VPO_8]_\infty$ chains perpendicular to the plane of projection.

The PO_4 tetrahedra are also significantly distorted compared to other monophosphates, with O–O distances that range from 2.33 to 2.58 Å and O–P–O angles from 95.7 to 114.8° (Table 4). Examination of the P–O distances show significant differences between the different kinds of PO_4 tetrahedra. The P(1) and P(4) tetrahedra, which are both linked to three VO_6 octahedra and one VO_5 pyramid, exhibit two different sets of distances, 1.52–1.53 and 1.50–1.56 Å, respectively; this difference between these two sorts of tetrahedra may be due to their being differently surrounded by lead ions, which establish much shorter Pb–O–P distances with the P(4) tetrahedra than with the P(1) tetrahedra. The P(2) tetrahedra appear more regular with O–O distances ranging from 2.43 to 2.58 Å, and four equal P–O bonds of 1.54 Å, despite the fact that they have one free apex, the three other apices being shared with VO_6 octahedra; this behavior may also be explained by the presence of lead ions which form two short Pb–O–P bonds with the free oxygen atoms of these tetrahedra. The P(3) tetrahedra are the most distorted, with O–O distances ranging from 2.33 to 2.58 Å and P–O bonds from 1.49 to 1.57 Å. This feature is explained by the fact that each P(3) tetrahedron shares one edge with a VO_5 pyramid and two apices with VO_6 octahedra, the fourth apex being free; consequently the two longer P–O distances of 1.57 Å correspond to triply bonded oxygens.

The lead ions, Pb(1) and Pb(2), are located in the [102] and [001] tunnels, respectively, at the intersection with the large obstructed tunnels running along [110] and [1$\bar{1}$0]. Pb(1) exhibits an eight fold coordination which can be described as a distorted rectangular prism. The four shorter Pb–O distances of 2.52–2.55 Å (Table 4) show that the four corresponding oxygen atoms O(16), O(13), $O(1^{vi})$, O(17) form approximately the basal plane of a tetragonal pyramid PbO_5L, whose fifth apex would correspond to the $6s^2$ lone pair of Pb(II). Pb(2) is characterized by a sevenfold coordination which can be described as a distorted pentagonal bipyramid. Again, in this polyhedron, the five closer neighbors with Pb–O distances ranging from 2.40 to 2.77 Å are located on the same side of Pb(2), leaving room for the $6s^2$ lone pair of Pb(II) in the opposite direction. The sum of the electrostatic valences calculated with the Brown–Altermatt curves (35) confirms the divalent state of lead. Moreover they indicate that the VO_6 octahedra are occupied by trivalent vanadium, whereas tetravalent vanadium is located in the VO_5 pyramid.

CONCLUDING REMARKS

The original structure of the vanadium monophosphate $Pb_2V_2VO(PO_4)_4$ confirms that, as in other mixed-valent V(IV)–V(III) phosphates, the V(III) and V(IV) species are distributed in an ordered way, i.e., exhibit an octahedral and a pyramidal coordination, respectively. This structural study also shows the great ability of V(III) and V(IV) to adopt a very distorted coordination. This suggests that it should be possible to generate numerous phosphates involving a mixed valence of vanadium.

REFERENCES

1. R. Gopal and C. Calvo, *J. Solid State Chem.* **5,** 432 (1972).
2. B. Jordan and C. Calvo, *Can. J. Chem.* **51,** 1621 (1973).
3. P. Amoros and D. Beltran-Porter, *Eur. J. Solid State Inorg. Chem.* **25,** 599 (1988).
4. K. Wang and K. H. Lii, *Acta Crystallogr. Sect. C* **48,** 975 (1992).
5. A. V. Lavrov, V. P. Nikolaev, G. G. Sadikow, and M. A. Porai-Koshits, *Sov. Phys. Dokl. Engl. Trans.* **27,** 680 (1982).
6. K. H. Lii and H. J. Tsai, *J. Solid State Chem.* **91,** 331 (1991).
7. K. H. Lii and S. L. Wang, *J. Solid State Chem.* **82,** 239 (1989).

8. A. Leclaire, H. Chahboun, D. Groult, and B. Raveau, *J. Solid State Chem.* **77,** 170 (1988).
9. K. H. Lii, H. J. Tsai, and S. L. Wang. *J. Solid State Chem.* **87,** 396 (1990).
10. K. H. Lii, Y. P. Wang, and S. L. Wang, *J. Solid State Chem.* **80,** 127 (1989).
11. K. H. Lii, Y. P. Wang, C. Y. Cheng, and S. L. Wang, *J. Chin. Chem. Soc. (Taipei)* **37,** 141 (1990).
12. C. C. Toraroi and J. C. Calabrese, *Inorg. Chem.* **23,** 1308 (1984).
13. J. W. Johnson, D. C. Johnson, A. J. Jacobson, and J. F. Brody, *J. Amer. Chem. Soc.* **106,** 8123 (1984).
14. N. G. Chernorukov, I. A. Korshunov, and N. P. Egorov, *Russian J. Inorg. Chem.* **23,** 1306 (1978).
15. C. A. Linde, I. E. Gorbunova, A. V. Lavrov, and V. E. Kutsnetsov, *Dokl. Akad. Nauk. SSSR* **244**(6) (1979).
16. A. Lebail, G. Ferey, P. Amoros, D. Beltran-Porter, and G. Villeneuve, *J. Solid State Chem.* **79,** 169 (1989).
17. L. Benhamada, A. Grandin, M. M. Borel, A. Leclaire, M. Leblanc, and B. Raveau, *J. Solid State Chem.* **96,** 390 (1992).
18. K. H. Lii, R. R. Chen, H. Y. Wang, and S. L. Wang, *J. Solid State Chem.* **99,** 72 (1992).
19. A. Grandin, J. Chardon, M. M. Borel, A. Leclaire, and B. Raveau, *J. Solid State Chem.* **99,** 277 (1992).
20. K. K. Palkina, S. I. Maksimova, N. T. Chibiskova, K. Schlesinger, and G. Ladwig, *Z. Anorg. Allg. Chem.* **529,** 89 (1985).
21. K. H. Lii, Y. P. Wang, Y. B. Chen, and S. L. Wang, *J. Solid State Chem.* **86,** 143 (1990).
22. L. Benhamada, A. Grandin, M. M. Borel, A. Leclaire, and B. Raveau, *Acta Crystallogr. C* **47,** 2437 (1991).
23. A. Benmoussa, M. M. Borel, A. Grandin, A. Leclaire, and B. Raveau, *J. Solid State Chem.* **97,** 314 (1992).
24. K. H. Lii, N. S. Wen, C. C. Su, and B. R. Chuch, *Inorg. Chem.* **31,** 439 (1992).
25. N. Casan, P. Amoros, R. Ibanez, E. Martinez-Tamayo, A. Beltran-Porter, and D. Beltran-Porter, *J. Inclusion Phenom.* **6**(2), 193 (1988).
26. S. L. Wang, H. Y. Kang, C. Y. Cheng, and K. H. Lii, *Inorg. Chem.* **30,** 3496 (1991).
27. K. H. Lii and C. S. Lee, *Inorg. Chem.* **29,** 3298 (1990).
28. L. Benhamada, A. Grandin, M. M. Borel, A. Leclaire, and B. Raveau, *J. Solid State Chem.* **97,** 131 (1992).
29. L. Benhamada, A. Grandin, M. M. Borel, A. Leclaire, and B. Raveau, *J. Solid State Chem.* **94,** 1274 (1991).
30. C. S. Lee, K. H. Lii, *J. Solid State Chem.* **92,** 362 (1991).
31. J. W. Johnson, D. C. Johnson, H. E. King, T. R. Halbert, J. F. Brody, D. P. Goshorn, *Inorg. Chem.* **27,** 1646 (1988).
32. P. Crespoa, A. Grandin, M. M. Borel, A. Leclaire, B. Raveau, *J. Solid State Chem.* **105,** 307 (1993).
33. M. M. Borel, M. Goreaud, A. Grandin, Ph. Labbe, A. Leclaire, B. Raveau, *Eur. J. Solid State Inorg. Chem.* **28,** 93 (1991).
34. G. Costentin, M. M. Borel, A. Grandin, A. Leclaire, and B. Raveau, *J. Solid State Chem.* **79,** 99 (1991).
35. I. D. Brown and D. Altermatt, *Acta. Crystallogr. Sect. B* **41,** 244 (1985).